

# Self-Similar acoustic white hole solutions in Bose-Einstein condensates and their Borel analysis

Sachin Vaidya<sup>1\*</sup>

<sup>1</sup> Dep. of Physics and Astronomy,  
Purdue University, W. Lafayette, IN

## Abstract

In this article, we study Self-Similar configurations of non-relativistic Bose-Einstein condensate (BEC) described by the Gross-Pitaevskii Equation (GPE). To be precise, we discuss singular Self-similar solutions of the Gross-Pitaevskii equation in 2D (with circular symmetry) and 3D (with spherical symmetry). We use these solutions to check for the crossover between the local speed of sound in the condensate and the magnitude of the flow velocity of the condensate, indicating the existence of a supersonic region and thus a sonic analog of a black-/white hole. This is because phonons cannot go against the condensate flow from the supersonic to the subsonic region in such a system. We also discuss numerical techniques used and study the semi-analytical Laplace-Borel resummation of asymptotic series solutions while making use of the asymptotic transseries to justify the choice of numerical and semi-analytical approaches taken.

---

\*E-mail: [vaidya2@purdue.edu](mailto:vaidya2@purdue.edu)

# Contents

<b>1</b>	<b>Introduction</b>	<b>2</b>
<b>2</b>	<b>Self similar solutions</b>	<b>4</b>
<b>3</b>	<b>Perturbative series Analysis</b>	<b>5</b>
3.1	Laplace-Borel Analysis . . . . .	9
<b>4</b>	<b>Numerical Solution</b>	<b>13</b>
<b>5</b>	<b>Fluctuations in the Self-Similar background solution</b>	<b>22</b>
<b>6</b>	<b>Self-Similar behavior</b>	<b>23</b>
<b>7</b>	<b>Conclusions</b>	<b>24</b>
<b>8</b>	<b>Acknowledgments</b>	<b>25</b>

## 1 Introduction

In [1] Unruh proposed studying Bose-Einstein condensates for gravitational analogs, which can be used to study phenomena such as Hawking radiation [2]. Such Bose-Einstein condensate models have been studied [3–8] in the past. Such models have also been developed in the cosmological context<sup>1</sup> (see [11], [12]) in the past. In this paper, we focus on developing a self-similar (scale invariant) analog gravity model from the Gross-Pitaevskii equation for non-relativistic BEC.

Self-Similarity (Scale Invariance) is studied in the context of various systems in Physics. Self-Similarity of the Gross-Pitaevskii equation (GPE) was studied earlier in [13]. Here we study a different type of self-similar configuration (with circular symmetry in 2D and spherical symmetry in 3D) in the Gross-Pitaevskii equation (GPE) that exhibits self-similarity in a combination of radial coordinate and time.

---

<sup>1</sup>Relativistic Bose-Einstein condensates can also be studied [9], [10]

To begin, we consider the Gross-Pitaevskii equation (GPE) with coupling  $g$  and without an external potential (see ref. [14]), describing the dynamics of a Bose-Einstein condensate (BEC)

$$i\hbar \frac{\partial \psi(\vec{\mathbf{r}}, t)}{\partial t} = -\frac{\hbar^2}{2m} \nabla^2 \psi(\vec{\mathbf{r}}, t) + g|\psi(\vec{\mathbf{r}}, t)|^2 \psi(\vec{\mathbf{r}}, t) \quad (1.1)$$

Small perturbations in the condensate can be shown to give an approximate local speed of sound in the long wavelength limit as (see ref. [15])

$$c(\vec{\mathbf{r}}, t) = \sqrt{\frac{n(\vec{\mathbf{r}}, t) g}{m}} \quad (1.2)$$

and similarly from the current density defined using the Gross-Pitaevskii equation, we can obtain the flow velocity (see ref. [16]) as follows

$$\vec{v}(\vec{\mathbf{r}}, t) = \frac{\vec{\mathbf{j}}(\vec{\mathbf{r}}, t)}{n(\vec{\mathbf{r}}, t)} = \frac{\hbar}{m} \vec{\nabla} \theta(\vec{\mathbf{r}}, t) \quad (1.3)$$

We use (1.1), (1.2), and (1.3) for a reference for the rest of the calculations. We focus on finding self-similar (in  $r$  and  $t$ ) solutions to the Gross-Pitaevskii equation (1.1) to look for solutions that can correspond to an acoustic black/white hole. It turns out that we cannot solve this problem analytically. Therefore, we study (in 2D) the perturbative series solution, which turns out to be factorially divergent, as we shall see. We use this series to demonstrate the utility of Laplace-Borel resummation to get an approximate self-similar solution from limited asymptotic data. Furthermore, we will also see that this series turns out to have non-perturbative corrections resulting in a transseries (see Ref. [17]), the properties of which we briefly discuss. We use this transseries to justify the use of the Runge-Kutta method of order four (RK4) [18] for numerical solutions.

## 2 Self similar solutions

To study the Self-Similar solutions with radial and time dependence, we write the Gross-Pitaevskii Equation (GPE) (1.1) in the form of scaled variables as

$$i \frac{\partial \chi(R, T)}{\partial T} = -\nabla_R^2 \chi(R, T) + |\chi(R, T)|^2 \chi(R, T) \quad (2.1)$$

where the scaled variables are

$$T = t, \quad (2.2)$$

$$R = \sqrt{\frac{2m}{\hbar}} r, \quad (2.3)$$

$$\chi(R, T) = \sqrt{\frac{g}{\hbar}} \psi(R, T), \quad (2.4)$$

$$\rho(R, T) = \sqrt{\frac{g}{\hbar}} \sqrt{n(R, T)} = \sqrt{\frac{g}{\hbar}} |\psi(R, T)| \quad (2.5)$$

It can be shown that the solution of the form  $\chi(R, T) = T^\alpha \zeta(R^\beta T^\gamma)$  (similar to [13]) exists if  $\alpha = -\frac{1}{2}$  and  $\gamma = -\frac{\beta}{2}$ . Changing the coordinates to  $v = \frac{R}{\sqrt{T}}$  and substituting

$$\chi(R, T) = \frac{1}{\sqrt{T}} \zeta(v) = \frac{1}{\sqrt{T}} \eta(v) \exp(i\theta(v)) \quad (2.6)$$

into (2.1), we get the imaginary part.

$$\left( 2 \frac{d\eta(v)}{dv} + \frac{\eta(v)(\mathbf{d}-1)}{v} \right) \left( \frac{d\theta(v)}{dv} \right) - \frac{v}{2} \frac{d\eta(v)}{dv} + \eta(v) \left( \frac{d^2\theta(v)}{dv^2} \right) - \frac{\eta(v)}{2} = 0 \quad (2.7)$$

and the real part

$$\frac{\mathbf{d}-1}{v} \left( \frac{d\eta(v)}{dv} \right) - \eta(v)^3 + \frac{d^2\eta(v)}{dv^2} - \eta(v) \left( \frac{d\theta(v)}{dv} \right)^2 + \frac{v\eta(v)}{2} \left( \frac{d\theta(v)}{dv} \right) = 0 \quad (2.8)$$

Although in  $\mathbf{d} = 3$  (2.7) does not have a closed-form solution, in  $\mathbf{d} = 2$  it does

have a closed-form solution as follows

$$\frac{d\theta(v)}{dv} = \frac{v}{4} + \frac{B}{v\eta(v)^2} \quad (2.9)$$

Furthermore, in the new scaled variables, the scaled local speed of sound (from (1.2)) becomes

$$C(R, T) = \sqrt{2}\rho(R, T) = \sqrt{2}|\chi(R, T)| = \sqrt{2}\frac{1}{\sqrt{T}}\eta\left(\frac{R}{\sqrt{T}}\right) = \sqrt{2}\frac{1}{\sqrt{T}}\eta(v) \quad (2.10)$$

and the scaled radial flow velocity (from (1.3)) of Bose-Einstein condensate (BEC) becomes

$$\bar{\mathbf{V}}(R, T) = 2\frac{\partial\theta(R, T)}{\partial R}\hat{\mathbf{R}} = 2\frac{\partial}{\partial R}\left(\theta\left(\frac{R}{\sqrt{T}}\right)\right)\hat{\mathbf{R}} = 2\frac{1}{\sqrt{T}}\frac{d(\theta(v))}{dv}\hat{\mathbf{R}} \quad (2.11)$$

### 3 Perturbative series Analysis

For  $\mathbf{d} = 2$ , equations (2.8) and (2.9) result in

$$\frac{d^2\eta(v)}{dv^2} + \frac{1}{v}\frac{d\eta(v)}{dv} + \frac{\eta(v)v^2}{16} - \frac{B^2}{\eta(v)^3v^2} - \eta(v)^3 = 0 \quad (3.1)$$

The asymptotic perturbative series solution of (3.1) can be written as follows.

$$\eta(v) = \frac{2\sqrt{B}}{v} \left( 1 + \left( B - \frac{1}{4} \right) \left( \frac{16}{v^4} + \left( \frac{9B}{2} - \frac{53}{8} \right) \frac{256}{v^8} + \left( \frac{55}{2}B^2 - \frac{535}{4}B + \frac{4447}{32} \right) \frac{4096}{v^{12}} + \dots \right) \right) \quad (3.2)$$

Since the solution must be real positive,  $B$  must be real positive to ensure that  $\sqrt{B}$  is real positive. It can be shown that the series coefficients have an alternating sign at large order. Also, as can be seen in Figures 1a and 1b, at large order  $\left| \frac{a_{n+1}}{a_n} \right| \approx \frac{(2(n+1))!}{(2n)!} \rightarrow 4n^2$  which means the coefficients grow like

$\approx (-1)^n (2n)!$  at large order up to a multiplying constant.

Note that the series lacks an arbitrary integration constant similar to the stationary singular solutions discussed in [19]. Asymptotically, the leading term in the solution goes like  $\frac{2\sqrt{B}}{v}$  as  $v \rightarrow \infty$  and therefore substituting  $\eta(v) = \frac{2\sqrt{B}(1+Af(v))}{v}$  into (3.1) and linearizing it in  $f(v)$  (see [20]), we get  $f(v) \approx \exp(\frac{\pm iv^2}{4}) + \dots$  where  $A$  represents two missing arbitrary constants of integration corresponding to  $\exp(\frac{+iv^2}{4})$  and  $\exp(\frac{-iv^2}{4})$  respectively. This reveals the arbitrary constants that were missing earlier. The functions  $\exp(\frac{\pm iv^2}{4})$  are non-perturbative as  $v \rightarrow \infty$  and they are finite oscillatory everywhere on the real  $v$  line meaning that they don't become singular. Therefore, none of the two arbitrary constants they bring in with them, has to be 0. Furthermore, since the differential equation is nonlinear in the dependent variable, non-perturbative corrections appear with ever-increasing powers and also bring in their own factorially divergent perturbative series multiplying them. This is how we end up with a two-parameter transseries (similar to [21] and [22]) on the real  $v$  line in this system. In addition to that, since the self-similar perturbative series has two types of non-perturbative corrections, there also turn out to be terms containing multiplications of these two types of non-perturbative corrections (instanton anti-instanton interactions).

With  $\eta(v) = \frac{2\sqrt{B}}{v}g(v)$  and a change of variable  $u = \frac{4}{v^2}$  in (3.2), we get

$$g(u) = 1 + \left(B - \frac{1}{4}\right) \left(u^2 + \left(\frac{9B}{2} - \frac{53}{8}\right)u^4 + \left(\frac{55}{2}B^2 - \frac{535}{4}B + \frac{4447}{32}\right)u^6\right) + \dots \quad (3.3)$$

and two-parameter transseries for this system (including (3.3)) with a first few terms turns out to be as follows:

$$\begin{aligned} g(u) = & 1 + \left(B - \frac{1}{4}\right) \left(u^2 + \left(\frac{9B}{2} - \frac{53}{8}\right)u^4 + \left(\frac{55}{2}B^2 - \frac{535}{4}B + \frac{4447}{32}\right)u^6\right) + \dots \\ & + C_1 e^{\frac{i}{u}} \left(1 + \frac{i(6B-1)u}{2} - \frac{3(12B^2-8B+1)u^2}{8} + \dots\right) \\ & + C_2 e^{\frac{-i}{u}} \left(1 - \frac{i(6B-1)u}{2} - \frac{3(12B^2-8B+1)u^2}{8} + \dots\right) \end{aligned}$$

$$\begin{aligned}
& + C_1 C_2 \left( 3 + \left( 18B - \frac{3}{4} \right) u^2 + \left( 159B^2 - 144B + \frac{159}{32} \right) u^4 + \dots \right) \\
& + \dots
\end{aligned} \tag{3.4}$$

where  $C_{1,2}$  are complex and  $C_2 = C_1^*$  to ensure that the transseries represents a real function<sup>2</sup>. Thus we still have two real free parameters in the transseries. There are no other constraints on these two real free parameters for the transseries solutions to be real. And therefore, we can set both the real parameters to 0 (effectively using (3.3)) to demonstrate the Laplace-Borel resummation in 2D without violating the reality condition on the solution, as shown in the subsequent section. On the other hand, setting these two real parameters to have any arbitrary nonzero values would result in oscillatory self-similar solutions with the oscillations of the form  $\exp(\frac{\pm i}{u}) = \exp(\frac{\pm i v^2}{4})$  as  $v \rightarrow \infty$  as we shall see. Furthermore, the freedom to choose two real free parameters (with zero or nonzero arbitrary values) for a second order ODE is equivalent to picking a function and its slope at any large  $v$  and solving the problem as an initial value problem using methods such as RK4 [18]. Therefore, numerically we solve this problem as an IVP using RK4 in C++.

In  $\mathbf{d} = 3$ , there is no closed-form solution for  $\frac{d\theta(v)}{dv}$ . However, in principle, a similar procedure as  $\mathbf{d} = 2$  can still be adopted. Here we make the simplest estimates as  $v \rightarrow \infty$  for the purposes of the numerical calculations.

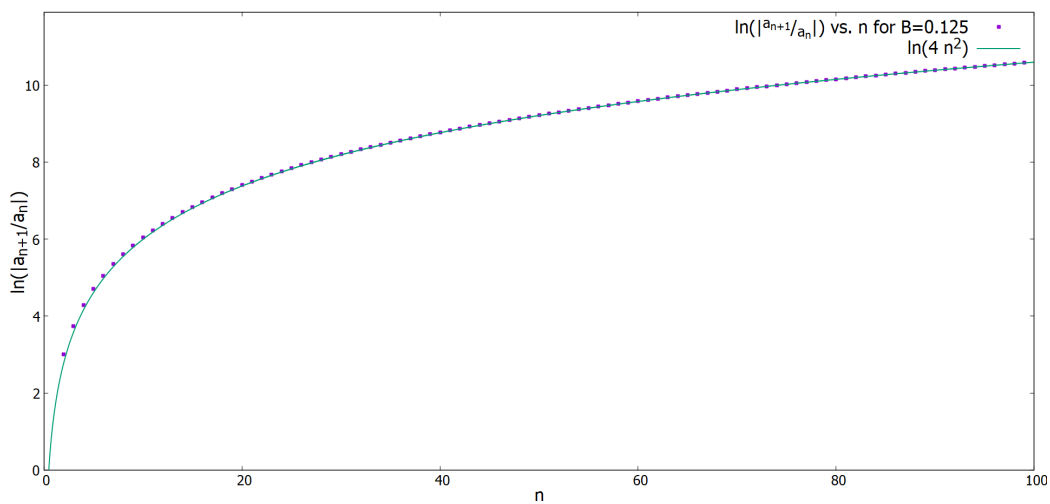
$$\begin{aligned}
\text{When } \eta(v) \approx \frac{C}{v} & \implies \frac{d\theta(v)}{dv} \approx \frac{2C^2}{v^3} \\
\text{and when } \eta(v) \approx \frac{C}{v^2} & \implies \frac{d\theta(v)}{dv} \approx \frac{v}{2}
\end{aligned} \tag{3.5}$$

where  $C > 0$  to ensure  $\eta(v) > 0$ . We use these conditions at large  $v$  as a reference to solve the initial value problem for a system of coupled ODEs in

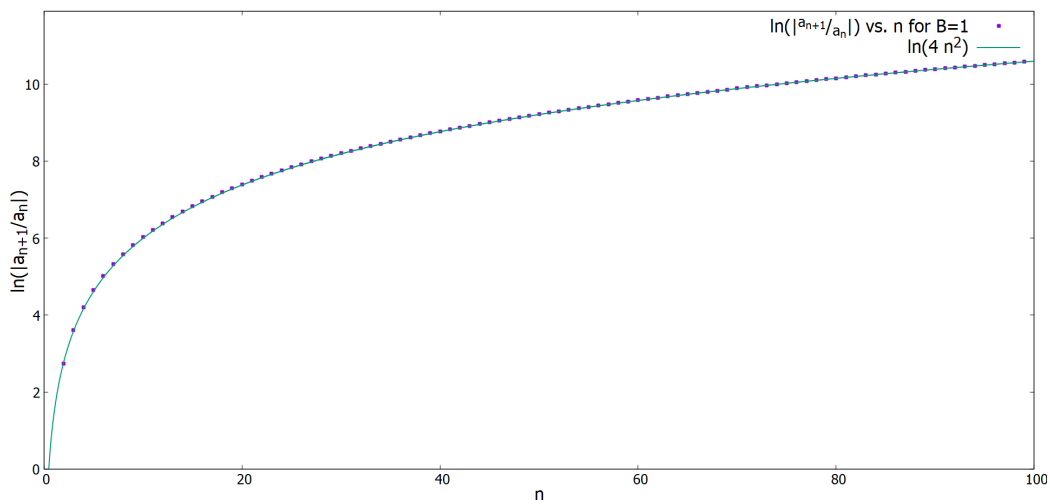
---

<sup>2</sup>Only few terms are displayed in the transseries here. However, in principle we can easily get first few hundred term using a software package such as Maple.

3D using RK4.



(a)  $B = 0.125$



(b)  $B = 1$

Figure 1: Sample plots of  $\ln\left(\left|\frac{a_{n+1}}{a_n}\right|\right)$  vs.  $n$  for Self Similar solutions in 2D



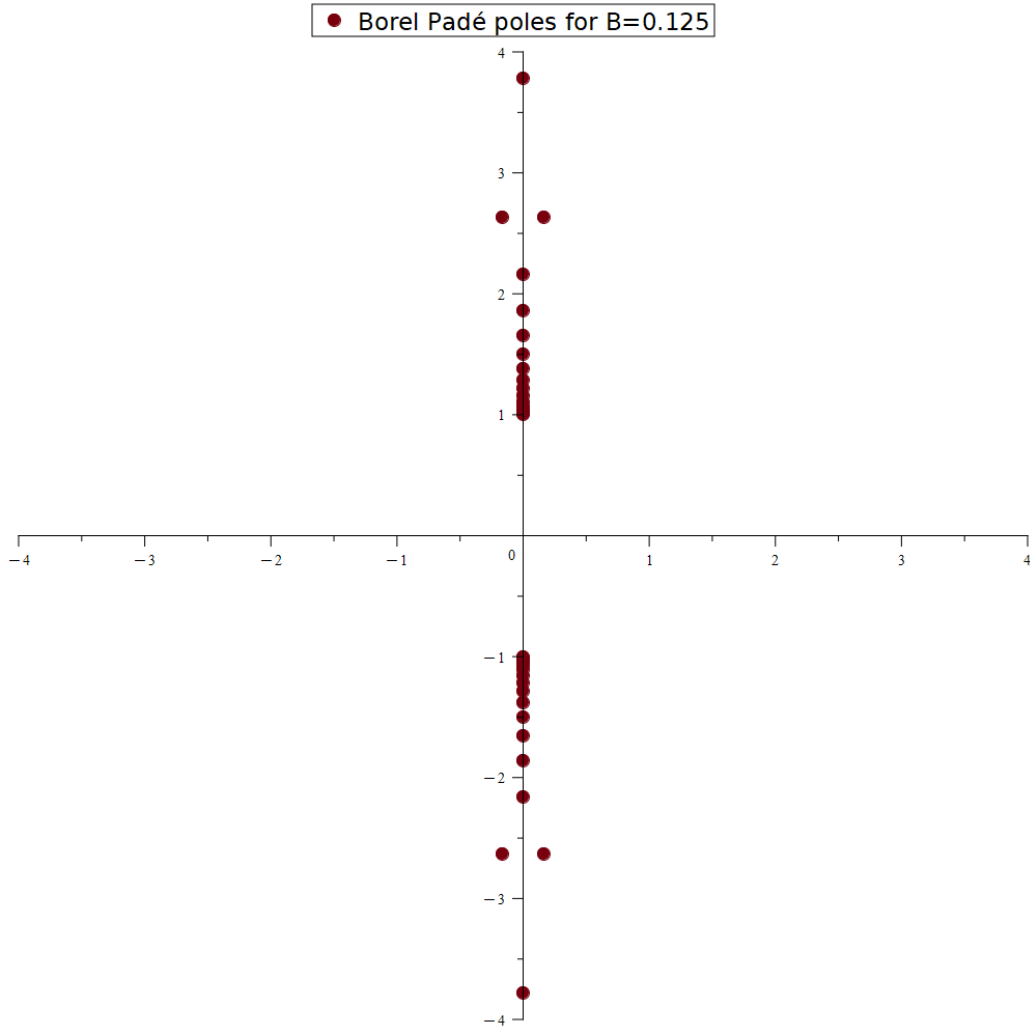


Figure 2: Approximate Borel Padé poles of Borel transform of (3.3) in  $U$  coordinate

### 3.1 Laplace-Borel Analysis

We evaluate the Borel transform<sup>3</sup> of  $\frac{g(u)}{(B-\frac{1}{4})}$  of order  $\mathcal{O}(U^{2b})$  from (3.3) and convert it into the Padé approximation or the Conformal Padé approximation using a procedure similar to Stationary solutions in [19]. Since the series

---

<sup>3</sup> $U$  is the Borel variable and we consider  $b = 100$  for these calculations

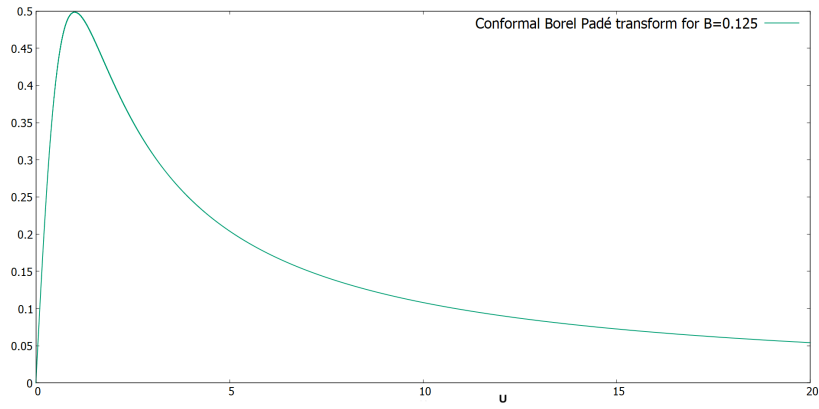
in (3.3), at large order, has factorially growing coefficients (see Fig. 1) with alternating sign, there is no singularity on the positive real  $U$  line in the Borel plane (similar to the Painlevé equation in [23]) as can be seen from the poles of the Borel Padé approximation of (3.3) in figure 2. Thus, the Laplace transform after the Borel Padé or the conformal Borel Padé transform does not have imaginary ambiguities containing real exponential functions (see [19] for reference). In addition to that, the non-perturbative corrections  $\left(\exp\left(\frac{\pm i}{u}\right) = \exp\left(\frac{\pm iv^2}{4}\right)\right)$  to the asymptotic perturbative series do not contain any real exponential functions and are finite. This indicates consistency. Therefore, no cancellation of imaginary non-perturbative ambiguities containing real exponents is needed for the solution to be real. Thus, for the purpose of demonstrating the Laplace-Borel resummation (see Fig. 4), we can restrict ourselves to solutions with both parameters of the transseries being 0, without violating the reality condition on  $\eta(v)$ .

For the actual calculations, similar to [19], we use conformal<sup>4</sup> Borel-Padé approximation<sup>5</sup> of  $(1+z^2)G(z)$  of order  $[b+1, b]$  where  $G(z)$  is the conformally mapped Borel transform of  $\frac{g(u)}{(B-\frac{1}{4})}$  of order  $\mathcal{O}(z^{2b})$ . Then we divide this result by  $(1+z^2)$  to get the actual conformal Borel-Padé transform of order  $[b+1, b+2]$  (see Fig. 3) of  $\frac{g(u)}{(B-\frac{1}{4})}$ , substitute  $z$  in terms of  $U$ , and Laplace integrate it on the real positive  $U$  line in the Borel plane. As is clearly evident from the conformal Borel-Padé transforms shown in Fig. 3, there is no singularity on the Laplace integration path in the Borel plane and therefore no singularity subtraction or contour deformation is needed, again indicating that there is no imaginary ambiguity in the Laplace integration result. Laplace integration is performed by integrating over  $U \in [0, 1]$  and over  $x = \frac{1}{U} \in [0, 1]$  to get the Laplace-Borel resummation result (see Fig. 4). Similarly, the Laplace-Borel resummation can also be done for  $\mathbf{d} = 3$  in principle.

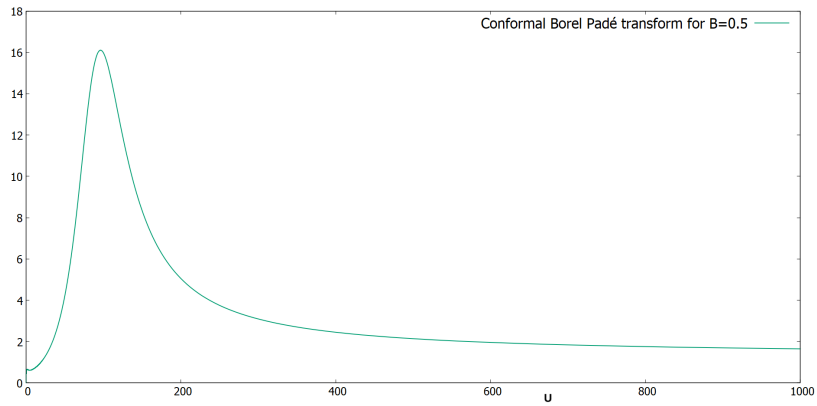
---

<sup>4</sup>With conformal map  $U = \frac{2z}{1-z^2}$  similar to [23]

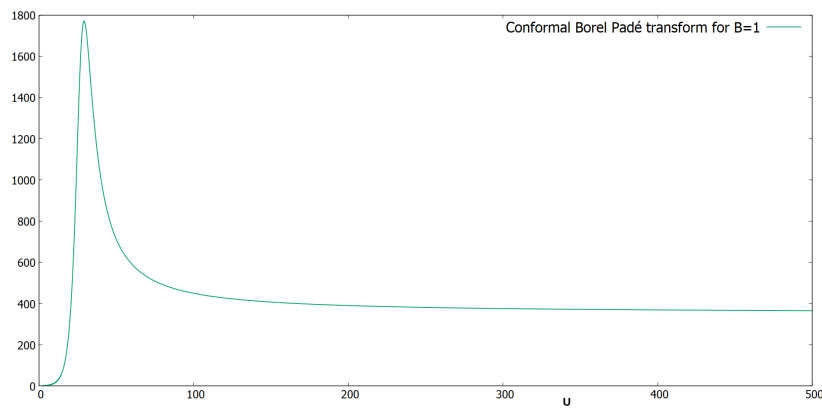
<sup>5</sup> $(1+z^2)$  because the  $g(u)$  series has even powers of  $u$  and the leading Borel singularities in variable  $z$  are at  $U = z = \pm i$



(a) Conformal Borel Padé transform for  $B = 0.125$

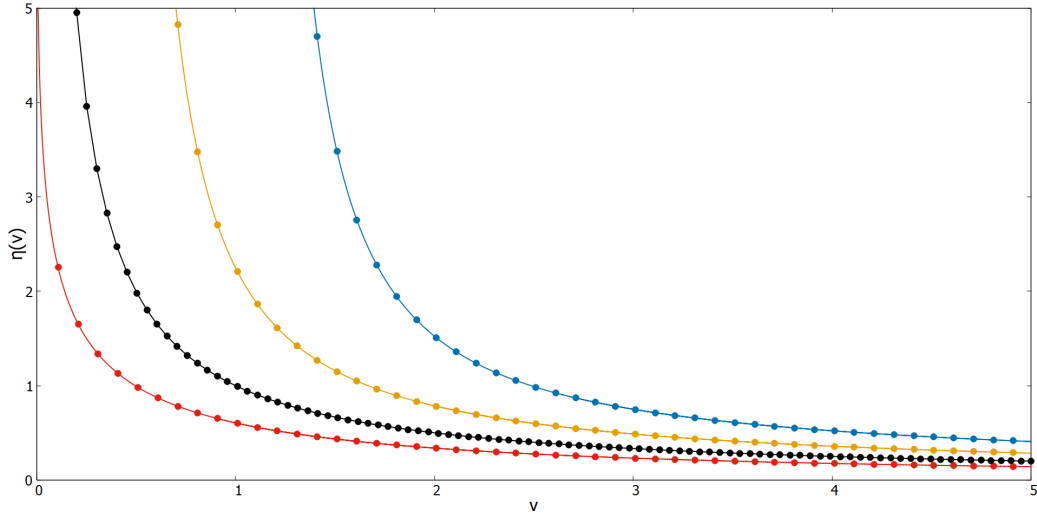


(b) Conformal Borel Padé transform for  $B = 0.5$

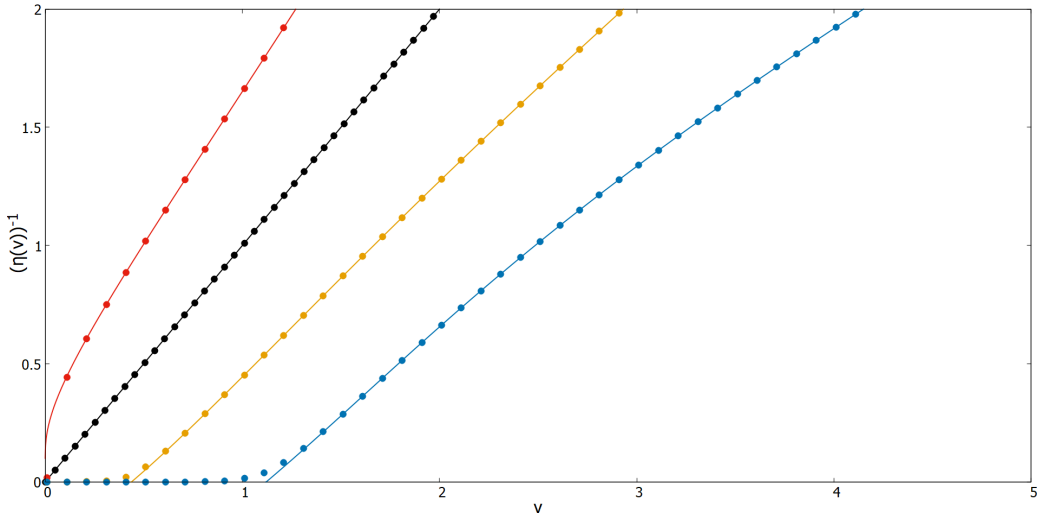


(c) Conformal Borel Padé transform for  $B = 1$

Figure 3: Conformal Borel Padé transforms for  $B = 0.125, 0.5, 1$  respectively in 2D



(a)  $\eta(v)$  vs.  $v$



(b)  $\frac{1}{\eta(v)}$  vs.  $v$

Figure 4: Initial value solution matched with Conformal Laplace-Borel transform for various values of parameter  $B$  in 2D. From left to right<sup>6</sup>  $B = 0.125, 0.25, 0.5, 1.0$ . The circles depict the resummed asymptotic series solution and the solid lines are the numerical solutions. In plot (b) we can see the discrepancy between the two for the same solutions when  $\rho \rightarrow \infty$  (near the horizontal axis where the series resummation fails).

<sup>6</sup>For  $B = 0.25$ ,  $g(u) = 1$  and therefore no Laplace Borel resummation is needed

## 4 Numerical Solution

Similar to the stationary case in [19], it can be shown that the governing differential equation (3.1) in 2D can have singular solutions for  $\eta(v)$ . To be precise, in 2D the singularity is of the form  $\eta(v) \approx \frac{1}{v}$  when it occurs at the origin, which gives  $\left. \frac{d\theta(v)}{dv} \right|_{v=0} = 0$ . And (in 2D) the singularity is of the form  $\eta(v) \approx \frac{\sqrt{2}}{v-v_0}$  when it occurs at  $v_0 > 0$ , which gives  $\left. \frac{d\theta(v)}{dv} \right|_{v=v_0} = \frac{v_0}{4}$ . This is in agreement with the initial value solution for  $\eta(v)$  starting from  $v = 100$  with different values of  $B$  (see Fig. 4) where the initial conditions are determined by the series (3.2). Logarithmically singular solution at  $v = 0$  is also possible in 2D, as can be seen for  $B = 0.125$  in Figure 4. For  $B = \frac{1}{4}$ , there exists an exact solution  $\eta(v) = \frac{1}{v}$  in 2D. We solve these ODEs as initial value problems starting from  $v = 100$  using RK4 [18] and initial conditions determined by the series (3.2) as shown for 2D in the Figure 4 for example. In 2D, Laplace-Borel resummation agrees well with the numerical solutions shown in Figure 4. Scaled speed of sound and magnitude of flow velocity for a sample solution (in 2D) with  $B = 1$  are shown in Figure 5.

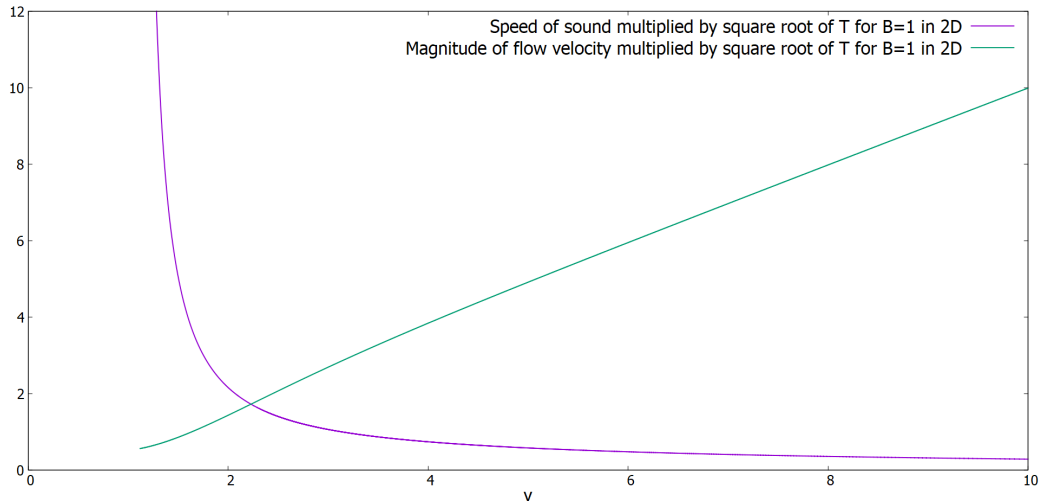
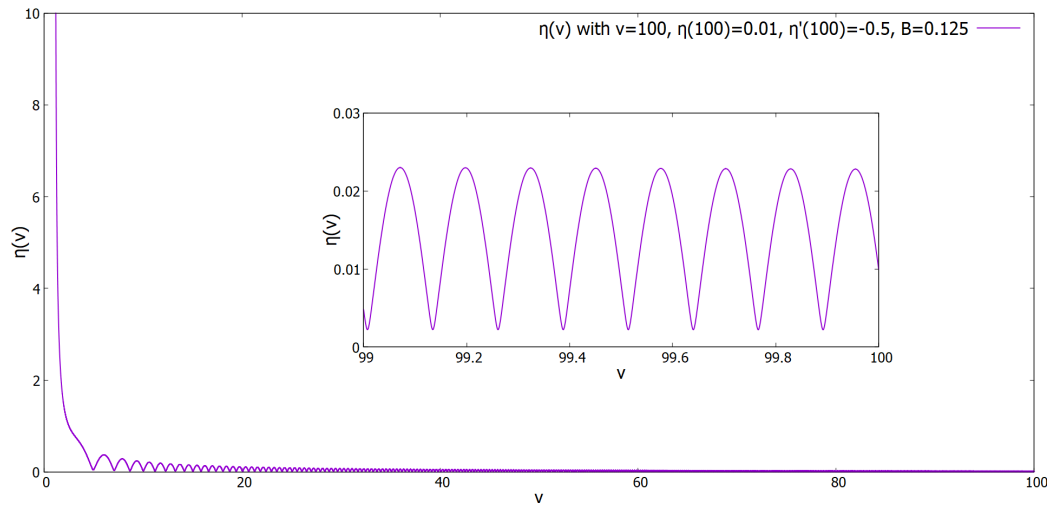
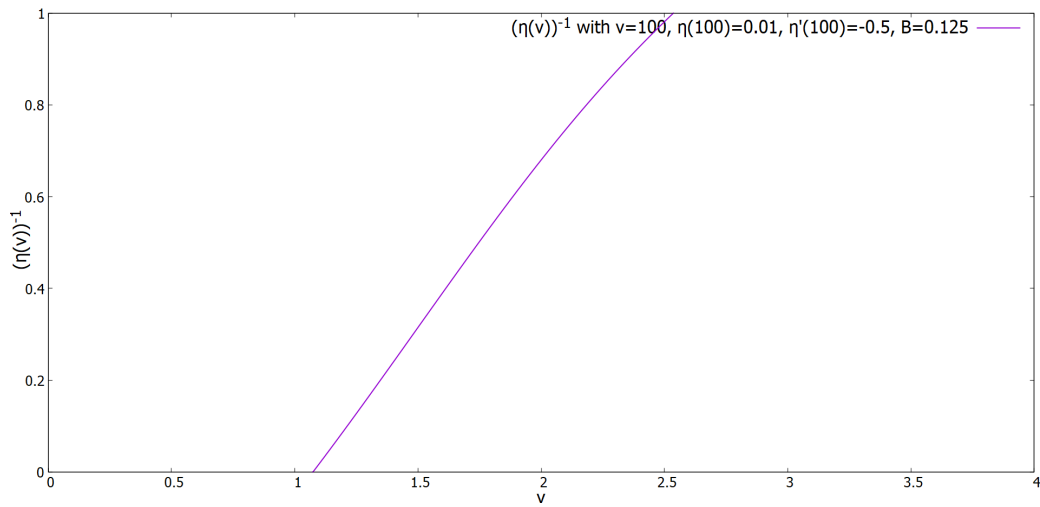


Figure 5: Scaled sound speed and flow speed of BEC in coordinate  $v$  for  $B = 1$  in 2D

The solutions (in 2D) discussed above are those with both transseries parameters being 0. However, we can also arbitrarily set the two parameters of the transseries subject to  $C_2 = C_1^*$  as we saw earlier in (3.4), which would be equivalent to setting the values of  $\eta(100)$  and  $\left. \frac{d\eta(v)}{dv} \right|_{v=100}$  that deviate from those given by equation (3.2). Then we can solve this initial value problem, the results of which are given in Figure 6. These solutions clearly have oscillations consistent with non-perturbative asymptotic corrections of the form  $\exp(\frac{\pm iv^2}{4})$  at large  $v$ . Note that the amplitude of the solution is of the form  $|\chi(R, T)| = \frac{1}{\sqrt{T}} \eta\left(\frac{R}{\sqrt{T}}\right)$ . This means that, when the singularity occurs at  $v_0 > 0$ , it will move outward in the  $R$  coordinate at the rate  $\sim \sqrt{T}$ . The only way to avoid this is to have a singularity that occurs at  $v = 0$ . This behavior exists for non-oscillatory solutions we found for  $B = \frac{1}{4}$  and  $B = \frac{1}{8}$ . To obtain oscillatory solutions with the singularity  $\frac{1}{v}$ , we solve the initial value problem for  $\frac{1}{\eta(v)} = \xi(v)$  with  $\xi(0.01) = 0.01$  and  $\left. \frac{d\xi(v)}{dv} \right|_{v=0.01} = 1$  that give  $\eta(v)$  as shown in Figure 7. It seems that the oscillatory singular solutions with  $\frac{1}{v}$  singularity exist only for  $B \leq 0.5$ . Similarly, if we picked the initial conditions from the series (3.2) at  $v = 100$  for  $B = 0.125$  for example, but set  $B$  in ODE (3.1) to some other small value (e.g.,  $B=0.1, 0.2$ ), we would get oscillatory solutions with logarithmic singularity as shown in Figure 8.

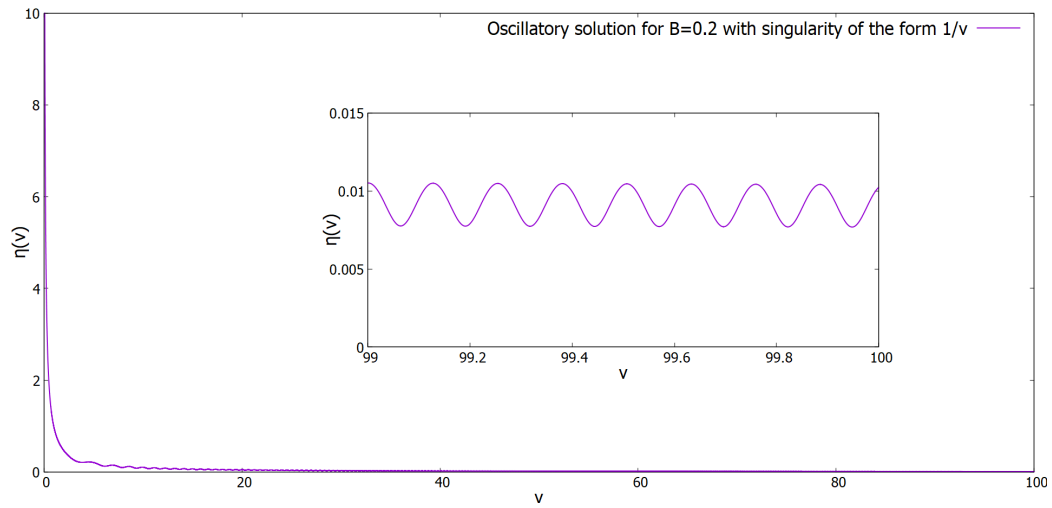


(a) Sample solution

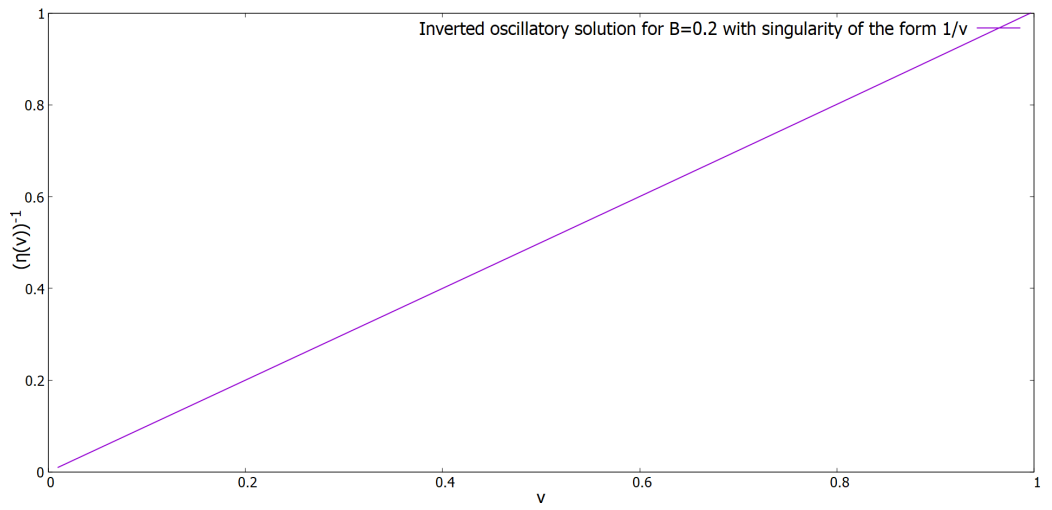


(b) Inverted sample solution

Figure 6: Sample oscillatory solution with singularity of the form  $\frac{\sqrt{2}}{v-v_0}$  in 2D



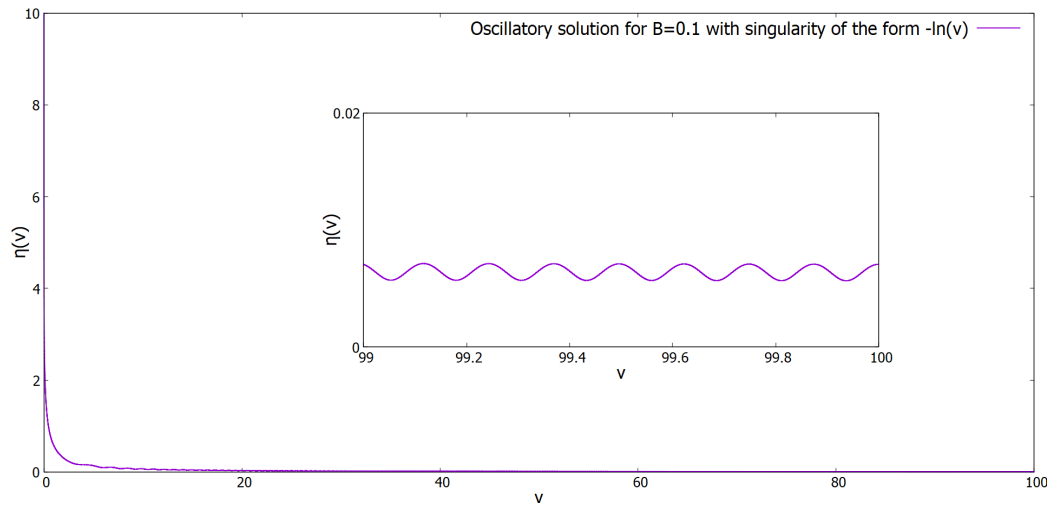
(a) Sample solution



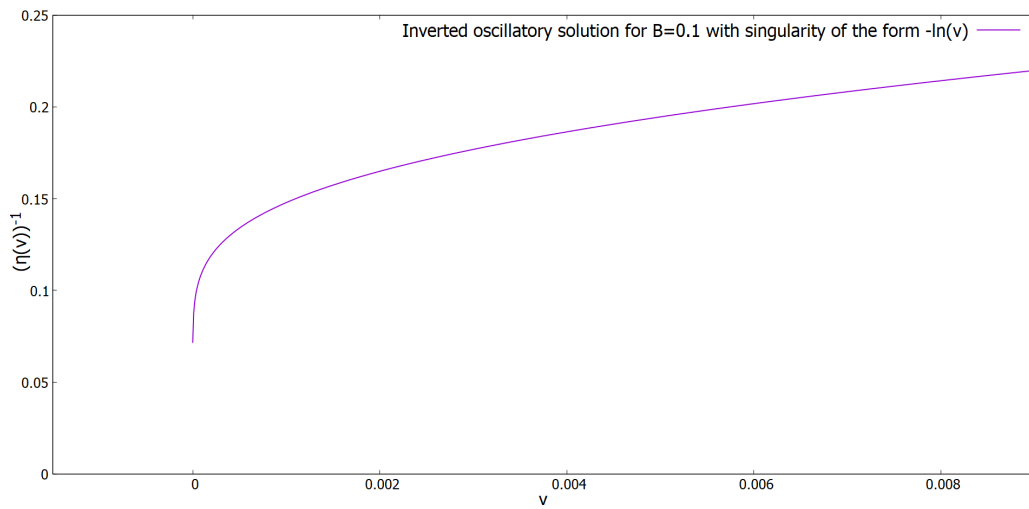
(b) Inverted sample solution

Figure 7: Sample oscillatory solution with singularity of the form  $\frac{1}{v}$  in 2D





(a) Sample solution



(b) Inverted sample solution

Figure 8: Sample oscillatory solution with logarithmic singularity at  $v = 0$  in 2D

Now if we consider the 3D case, similar to the stationary case in [19], it can be shown that the governing differential equations (2.8) and (2.7) in 3D can also have singular solutions for  $\eta(v)$ . It can be shown that when the singularity occurs at some  $v_0 > 0$ , it is of the form  $\frac{\sqrt{2}}{v-v_0}$  and should give  $\frac{d\theta(v)}{dv}\Big|_{v=v_0} = \frac{v_0}{4}$ . This is consistent with the result of the initial value problem. The initial value problem for a system of coupled ODEs (2.8) and (2.7) is solved with approximate initial conditions given by (3.5) starting from  $v = 100$  using RK4 [18]. Sample solutions (in 3D) with  $C = 1$  are shown in Figure 9. Similar to the 2D case, even in 3D if we choose initial conditions (at  $v = 100$ ) deviating from the ones discussed in (3.5), we see similar oscillatory behavior that appears to have oscillations of the form  $\exp(\frac{\pm iv^2}{4})$  at large  $v$ , as can be seen in Figure 10. For the same reason as 2D, we also find (oscillatory) singular solutions in 3D with singularity at  $v \approx 0$ , by trial and error (Figure 11).

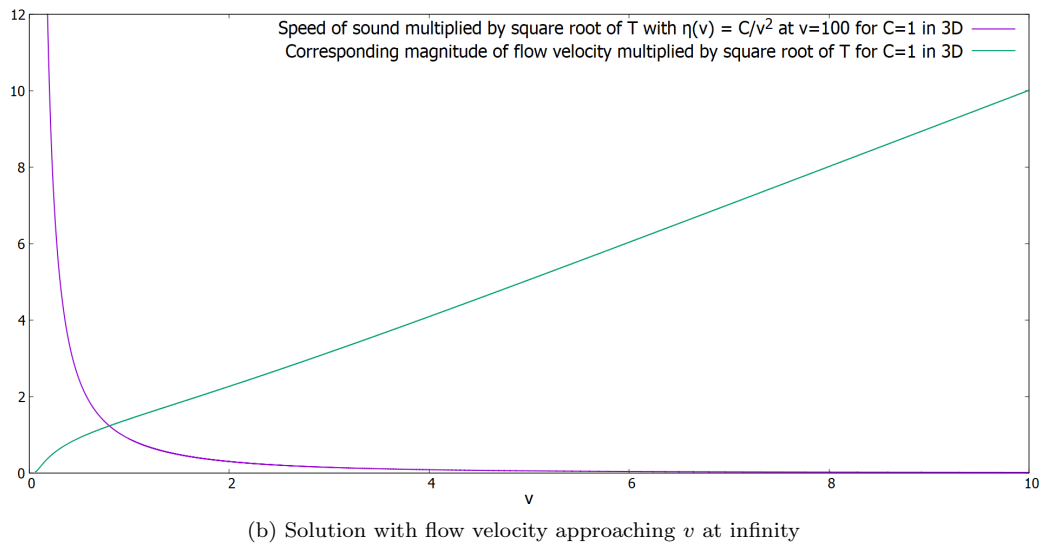
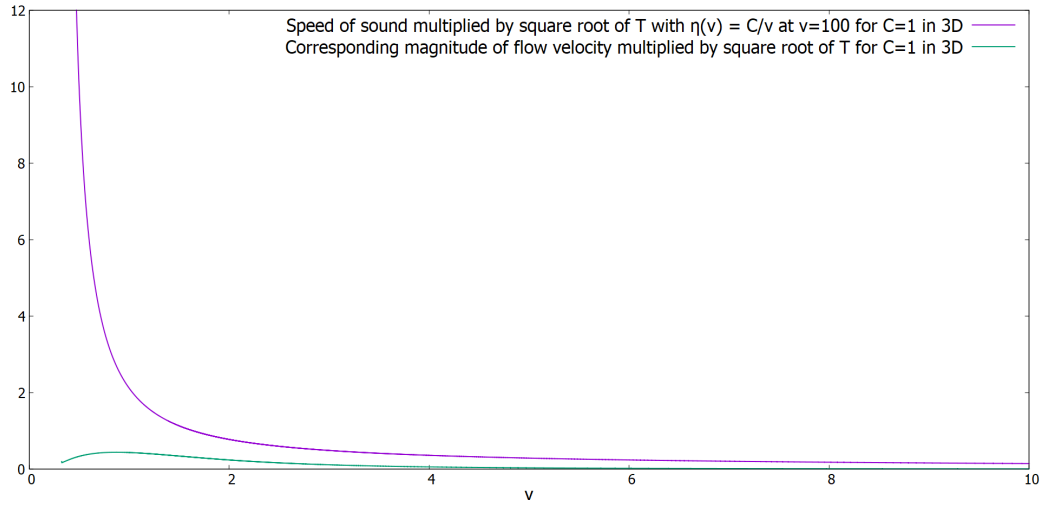
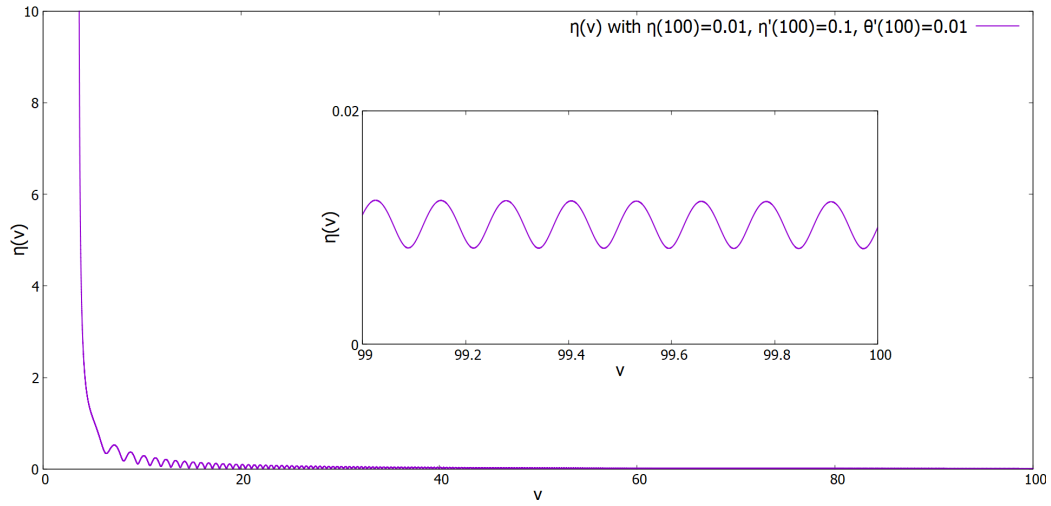
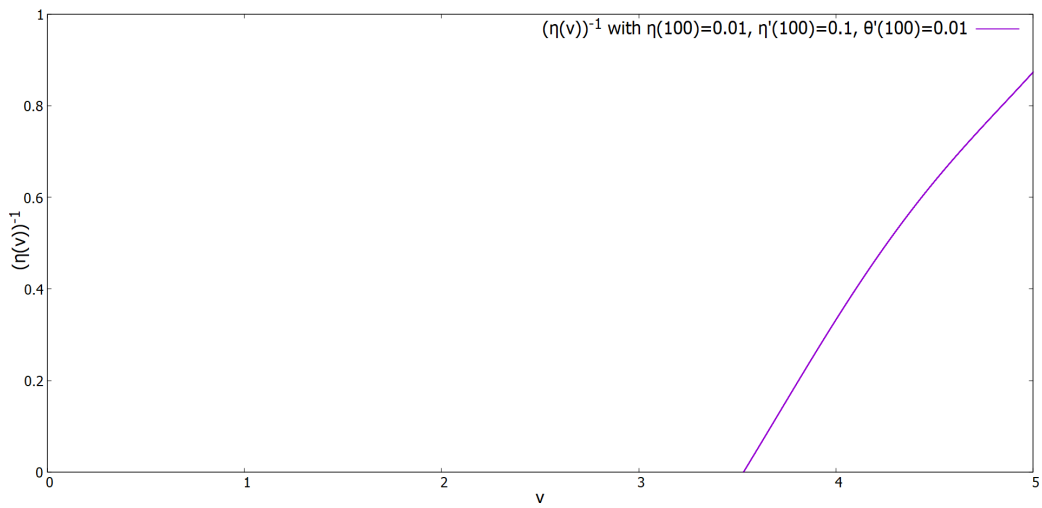


Figure 9: Scaled sound speed and flow speed of BEC in coordinate  $v$  for  $C = 1$  in 3D

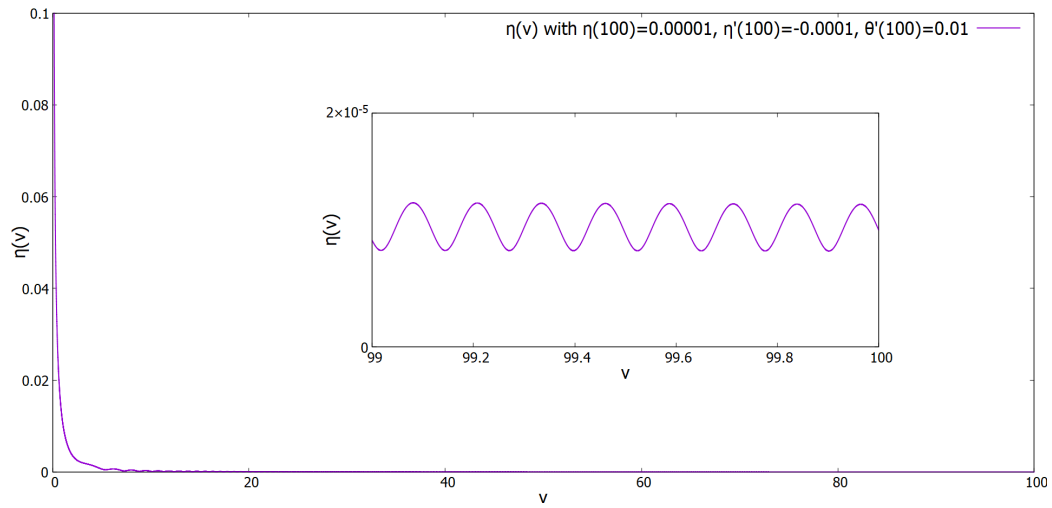


(a) Sample solution

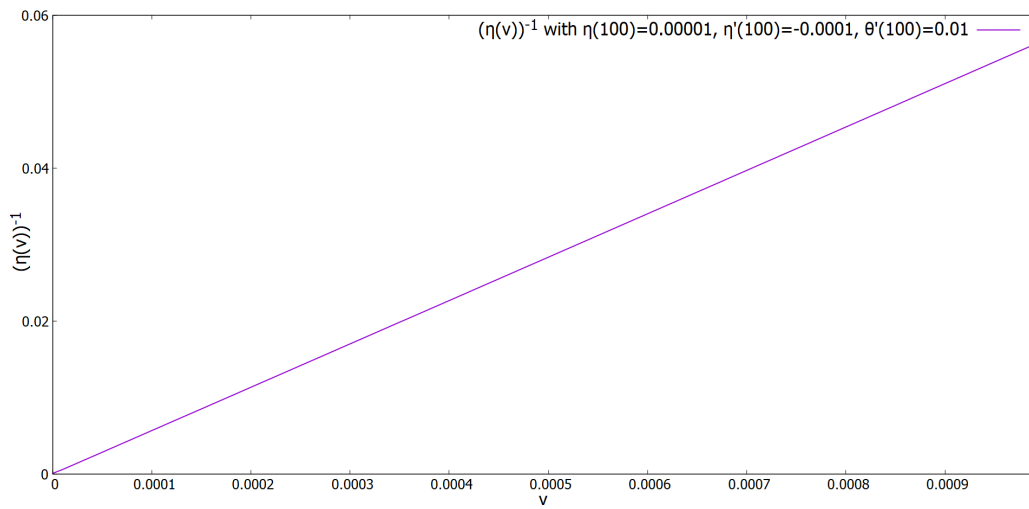


(b) Inverted sample solution

Figure 10: Sample oscillatory solution with singularity of the form  $\frac{\sqrt{2}}{v-v_0}$  in 3D



(a) Sample solution



(b) Inverted sample solution

Figure 11: Sample (oscillatory) solution with singularity at  $v \approx 0$  in 3D

## 5 Fluctuations in the Self-Similar background solution

We can also study the dynamics of fluctuations in the background phase and amplitude (Self-Similar) solutions by writing the fluctuations as follows

$$\begin{aligned}
\chi(\vec{\mathbf{R}}, T) &= \sqrt{n(\vec{\mathbf{R}}, T)} \exp(i\theta(\vec{\mathbf{R}}, T)) \\
&= \sqrt{n_0(T, R) + n_1(\vec{\mathbf{R}}, T)} \exp(i(\theta_0(T, R) + \theta_1(\vec{\mathbf{R}}, T))) \\
&= \sqrt{n_0(T, R)} \exp(i\theta_0(T, R)) (1 + N_1(\vec{\mathbf{R}}, T) + i\theta_1(\vec{\mathbf{R}}, T)) \quad (5.1)
\end{aligned}$$

where  $N_1(\vec{\mathbf{R}}, T) = \frac{n_1(\vec{\mathbf{R}}, T)}{2n_0(T, R)}$ . Here,  $n_0(T, R) = (\rho_0(T, R))^2 = \left(\frac{1}{\sqrt{T}}\eta\left(\frac{R}{\sqrt{T}}\right)\right)^2$  and  $\theta_0(T, R) = \theta_0\left(\frac{R}{\sqrt{T}}\right)$  are the background density and phase respectively. Additionally,  $\vec{\mathbf{R}}$  is  $(R, \varphi)$  in 2D and  $(R, \theta, \varphi)$  in 3D.

Substituting (5.1) into equation (2.1), we get the real and imaginary parts of the linearized equations as follows

$$(\partial_T \pm |\vec{\mathbf{V}}(R, T)|\partial_R) N_1(\vec{\mathbf{R}}, T) = -\frac{1}{C(T, R)^2} \nabla_R \cdot (C(T, R)^2 \nabla_R \theta_1(\vec{\mathbf{R}}, T)) \quad (5.2)$$

$$\begin{aligned}
(\partial_T \pm |\vec{\mathbf{V}}(R, T)|\partial_R) \theta_1(\vec{\mathbf{R}}, T) &= \frac{1}{C(T, R)^2} \nabla_R \cdot (C(T, R)^2 \nabla_R N_1(\vec{\mathbf{R}}, T)) \\
&\quad - C(T, R)^2 N_1(\vec{\mathbf{R}}, T) \quad (5.3)
\end{aligned}$$

where,  $N_1(\vec{\mathbf{R}}, T) = \frac{n_1(\vec{\mathbf{R}}, T)}{2n_0(T, R)} = \frac{n_1(\vec{\mathbf{R}}, T)}{2(\rho_0(T, R))^2} = \frac{n_1(\vec{\mathbf{R}}, T)}{(C(T, R))^2}$  and  $\rho_0(T, R) = \frac{1}{\sqrt{T}}\eta\left(\frac{R}{\sqrt{T}}\right)$ . Furthermore, it is easy to show under the change of coordinate  $v = \frac{R}{\sqrt{T}}$  that the equations (5.2) and (5.3) also exhibit self-similarity, and hence the phase fluctuations and density fluctuations are also self-similar and thus are static sinusoids in the  $v = \frac{R}{\sqrt{T}}$  coordinate.

Under the hydrodynamic approximation  $\nabla_R \cdot (C(T, R)^2 \nabla_R N_1(\vec{\mathbf{R}}, T)) \approx 0$  (see [4] and [5]), equations (5.2) and (5.3) can be combined into a wave equation that looks like a massless scalar field  $\theta_1(\vec{\mathbf{R}}, T)$  in a (analog) space-time background. Corresponding analog space-time metric (see [24]) in 2D turns out to be

$$g_{\mu\nu} \sim (C(T, R))^4 \begin{bmatrix} -\left(1 - \frac{(|\vec{\mathbf{V}}(T, R)|)^2}{(C(T, R))^2}\right) \mp \frac{|\vec{\mathbf{V}}(T, R)|}{(C(T, R))^2} & 0 \\ \mp \frac{|\vec{\mathbf{V}}(T, R)|}{(C(T, R))^2} & \frac{1}{(C(T, R))^2} \\ 0 & 0 \\ 0 & \frac{R^2}{(C(T, R))^2} \end{bmatrix} \quad (5.4)$$

and analog space-time metric in 3D turns out to be

$$g_{\mu\nu} \sim (C(T, R))^3 \begin{bmatrix} -\left(1 - \frac{(|\vec{\mathbf{V}}(T, R)|)^2}{(C(T, R))^2}\right) \mp \frac{|\vec{\mathbf{V}}(T, R)|}{(C(T, R))^2} & 0 & 0 \\ \mp \frac{|\vec{\mathbf{V}}(T, R)|}{(C(T, R))^2} & \frac{1}{(C(T, R))^2} & 0 \\ 0 & 0 & \frac{R^2 \sin^2(\theta)}{(C(T, R))^2} \\ 0 & 0 & 0 & \frac{R^2}{(C(T, R))^2} \end{bmatrix} \quad (5.5)$$

where, “−” sign for outward flow and “+” sign for inward flow. Note that (5.4) and (5.5) resemble the Schwarzschild metric in Painlevé-Gullstrand coordinates (see [25]). We consider “−” sign in the acoustic metric tensors above because these are the solutions with crossover between local speed of sound and flow speed indicating an acoustic (white hole) horizon.

## 6 Self-Similar behavior

We see that self-similar non-oscillatory solutions seem to have outward flow velocity indicating a sonic analog of a white hole when there is a crossing between flow speed and sound speed. The same is the case with some self-

similar oscillatory solutions<sup>7</sup>. It is easy to see that the functions  $\eta(v)$  and  $\frac{d}{dv}(\theta(v))$  appear to be fixed in coordinate  $v$ . This indicates that all functions (in the solution) in  $v$ , when mapped back to the coordinate  $R$ , move radially outwards (especially oscillatory ones in the form of sinusoidal waves) with time at the rate  $\propto \sqrt{T}$ . Furthermore, from  $\frac{\sqrt{2}}{\sqrt{T}}\eta(v)$  and  $\frac{2}{\sqrt{T}}\frac{d}{dv}(\theta(v))$ , all amplitudes, sound speed, and flow velocity clearly also decay with time at the rate  $\propto \frac{1}{\sqrt{T}}$ . Furthermore, since the flow is always outgoing in 2D and 3D, when there is a crossing between the approximate local speed of sound and the magnitude of the flow velocity, there is a white hole horizon that remains at a constant  $v$  defined by  $(2\frac{d}{dv}(\theta(v))\hat{\mathbf{R}})^2 - (\sqrt{2}\eta(v))^2 = 0$  from (5.4), (5.5), (2.10), and (2.11). Therefore, the radius of the horizon grows as  $R_h \propto \sqrt{T}$ .

## 7 Conclusions

In this article, we studied Self-Similar (in radial coordinate and time) configurations of non-relativistic Bose-Einstein condensate (BEC) described by the Gross-Pitaevskii Equation (GPE). The (singular) self-similar solutions in this model in 2D (with circular symmetry) and 3D (with spherical symmetry) have outward flow velocity, and it crosses the scaled local speed of sound, clearly indicating the existence of a sonic analog of a white hole. Particularly in 3D, this crossing occurs in the case of the solutions with flow velocity growing radially outward. Since the flow remains supersonic everywhere outside the horizon and keeps getting faster with radial distance, this model is more relevant for analog models in a cosmological context (see [11], [12] for example) in the non-relativistic limit. Furthermore, the white hole horizon grows at the rate  $R_h \propto \sqrt{T}$  as we saw. Also, the oscillatory solutions appear like sinusoidal waves moving outward at the rate of  $\sqrt{T}$  while simultaneously being suppressed by the factor of  $\frac{1}{\sqrt{T}}$ . We also find that the linearized equa-

---

<sup>7</sup>They correspond to the transseries with at least one of the two real transseries parameters being nonzero as discussed earlier.



tions governing fluctuations as well as the acoustic metric tensors also exhibit this self-similarity.

In 2D, we also check the Transseries<sup>8</sup> as  $v = \frac{R}{\sqrt{T}} \rightarrow \infty$  and demonstrate how its Laplace-Borel resummation matches well with the numerical solutions obtained from the Runge-Kutta method of order four (RK4). We show how Laplace-Borel resummation can be used to extract information about the solutions even at smaller  $v = \frac{R}{\sqrt{T}}$  values from the limited amount of information available at  $v = \frac{R}{\sqrt{T}} \rightarrow \infty$ .

## 8 Acknowledgments

I am grateful to the DOE for support under the Fermilab Quantum Consortium. I would like to thank my PhD advisor, Dr. Luis M. Kruczenski, for his guidance and support for this project. I wish to acknowledge valuable discussions with Akilesh Venkatesh and Kunaal Joshi on numerical techniques. I also wish to acknowledge valuable computational resources provided by RCAC (Rosen Center For Advanced Computing) at Purdue University.

## References

- [1] W. G. Unruh. “Experimental Black-Hole Evaporation?” In: *Phys. Rev. Lett.* 46 (21 May 1981), pp. 1351–1353.
- [2] S. W. Hawking. “Particle creation by black holes”. eng. In: *Commun. Math. Phys.*, v. 43, no. 3, pp. 199–220 43.3 (1975), pp. 199–220. ISSN: 0010-3616.
- [3] Carlos Barceló, Stefano Liberati, and Matt Visser. “Analogue Gravity”. In: *Living Reviews in Relativity* 14.1 (May 2011), p. 3. ISSN: 1433-8351.

---

<sup>8</sup>With both (real) transseries parameters set to 0 for the reasons explained earlier.

- [4] Carlos Barceló, S Liberati, and Matt Visser. “Analogue gravity from Bose-Einstein condensates”. In: *Classical and Quantum Gravity* 18.6 (Mar. 2001), p. 1137.
- [5] Matt Visser, Carlos Barceló, and Stefano Liberati. “Analogue Models of and for Gravity”. In: *General Relativity and Gravitation* 34.10 (Oct. 2002), pp. 1719–1734. ISSN: 1572-9532.
- [6] L. J. Garay et al. “Sonic Analog of Gravitational Black Holes in Bose-Einstein Condensates”. In: *Phys. Rev. Lett.* 85 (22 Nov. 2000), pp. 4643–4647.
- [7] Caio C. Holanda Ribeiro, Sang-Shin Baak, and Uwe R. Fischer. “Existence of steady-state black hole analogs in finite quasi-one-dimensional Bose-Einstein condensates”. In: *Phys. Rev. D* 105 (12 June 2022), p. 124066.
- [8] Zehua Tian et al. “Testing the upper bound on the speed of scrambling with an analogue of Hawking radiation using trapped ions”. In: *The European Physical Journal C* 82.3 (2022), p. 212. ISSN: 1434-6052.
- [9] I. Dymnikova and M. Khlopov. “Decay of cosmological constant in self-consistent inflation”. In: *The European Physical Journal C - Particles and Fields* 20.1 (Apr. 2001), pp. 139–146. ISSN: 1434-6052.
- [10] IRINA DYMNIKOVA and MAXIM KHLOPOV. “DECAY OF COSMOLOGICAL CONSTANT AS BOSE CONDENSATE EVAPORATION”. In: *Modern Physics Letters A* 15.38n39 (2000), pp. 2305–2314.
- [11] Petr O. Fedichev and Uwe R. Fischer. ““Cosmological” quasiparticle production in harmonically trapped superfluid gases”. In: *Phys. Rev. A* 69 (3 Mar. 2004), p. 033602.
- [12] Petr O. Fedichev and Uwe R. Fischer. “Gibbons-Hawking Effect in the Sonic de Sitter Space-Time of an Expanding Bose-Einstein-Condensed Gas”. In: *Phys. Rev. Lett.* 91 (24 Dec. 2003), p. 240407.

- [13] Imre F. Barna, Mihály A. Pocsai, and L. Mátyás. “Self-Similarity Analysis of the Nonlinear Schrödinger Equation in the Madelung Form”. In: *Advances in Mathematical Physics* 2018 (Oct. 2018), p. 7087295. ISSN: 1687-9120.
- [14] P. Nozieres and D. Pines. *The Theory of Quantum Liquids: Superfluid Bose Liquids*. Advanced book Classics. Westview Press, pp. 160–161. ISBN: 0201408414.
- [15] P. Nozieres and D. Pines. *The Theory of Quantum Liquids: Superfluid Bose Liquids*. Advanced book Classics. Westview Press, pp. 168–169. ISBN: 0201408414.
- [16] P. Nozieres and D. Pines. *The Theory of Quantum Liquids: Superfluid Bose Liquids*. Advanced book Classics. Westview Press, p. 66. ISBN: 0201408414.
- [17] Ovidiu Costin. “Exponential asymptotics, transseries, and generalized Borel summation for analytic, nonlinear, rank-one systems of ordinary differential equations”. In: *International Mathematics Research Notices* 1995.8 (Apr. 1995), pp. 377–417. ISSN: 1073-7928.
- [18] Ernst Hairer and Gerhard Wanner. “Runge–Kutta Methods, Explicit, Implicit”. In: *Encyclopedia of Applied and Computational Mathematics*. Ed. by Björn Engquist. Berlin, Heidelberg: Springer Berlin Heidelberg, 2015, pp. 1282–1285. ISBN: 978-3-540-70529-1.
- [19] Sachin Vaidya and Martin Kruczenski. *Stationary acoustic black hole solutions in Bose-Einstein condensates and their Borel analysis*. 2024. arXiv: 2411.06678 [cond-mat.quant-gas].
- [20] O. Costin, R. D. Costin, and M. Huang. “Tronquée Solutions of the Painlevé Equation P<sub>I</sub>”. In: *Constructive Approximation* 41.3 (June 1, 2015), pp. 467–494. ISSN: 1432-0940.

- [21] Inês Aniceto and Ricardo Schiappa. “Nonperturbative Ambiguities and the Reality of Resurgent Transseries”. In: *Communications in Mathematical Physics* 335.1 (Apr. 2015), pp. 183–245. ISSN: 1432-0916.
- [22] Stavros Garoufalidis et al. “Asymptotics of the Instantons of Painlevé I”. In: *International Mathematics Research Notices* 2012.3 (Mar. 2011), pp. 561–606. ISSN: 1073-7928.
- [23] Ovidiu Costin and Gerald V Dunne. “Resurgent extrapolation: rebuilding a function from asymptotic data. Painlevé I”. In: *Journal of Physics A: Mathematical and Theoretical* 52.44 (Oct. 2019), p. 445205.
- [24] L. J. Garay et al. “Sonic black holes in dilute Bose-Einstein condensates”. In: *Phys. Rev. A* 63 (2 Jan. 2001), p. 023611.
- [25] Andrew J. S. Hamilton and Jason P. Lisle. “The river model of black holes”. eng. In: *American journal of physics* 76.6 (2008), pp. 519–532. ISSN: 0002-9505.